

Composition and concentration anomalies for structure and dynamics of Gaussian-core mixtures

Mark J. Pond,^{1,*} William P. Krekelberg,¹ Vincent K. Shen,^{2,†} Jeffrey R. Errington,^{3,‡} and Thomas M. Truskett^{1,4,§}

¹*Department of Chemical Engineering, University of Texas at Austin, Austin, TX 78712.*

²*Physical and Chemical Properties Division, National Institute of Standards and Technology, Gaithersburg, Maryland 02899-8380, USA*

³*Department of Chemical and Biological Engineering, University at Buffalo, The State University of New York, Buffalo, New York 14260-4200, USA*

⁴*Institute for Theoretical Chemistry, University of Texas at Austin, Austin, TX 78712.*

We report molecular dynamics simulation results for two-component fluid mixtures of Gaussian-core particles, focusing on how tracer diffusivities and static pair correlations depend on temperature, particle concentration, and composition. At low particle concentrations, these systems behave like simple atomic mixtures. However, for intermediate concentrations, the single-particle dynamics of the two species largely decouple, giving rise to the following anomalous trends. Increasing either the concentration of the fluid (at fixed composition) or the mole fraction of the larger particles (at fixed particle concentration) enhances the tracer diffusivity of the larger particles, but decreases that of the smaller particles. In fact, at sufficiently high particle concentrations, the larger particles exhibit higher mobility than the smaller particles. Each of these dynamic behaviors is accompanied by a corresponding structural trend that characterizes how either concentration or composition affects the strength of the static pair correlations. Specifically, the dynamic trends observed here are consistent with a single empirical scaling law that relates an appropriately normalized tracer diffusivity to its pair-correlation contribution to the excess entropy.

Fluids of identical particles interacting via the Gaussian-core (GC) pair potential have been the subject of many recent investigations.^{1,2,3,4,5,6,7,8,9} Continued interest in this model system, introduced by Stillinger in 1976,¹⁰ can be attributed in part to the fact that the GC potential is a simple and computationally tractable idealization of the soft, effective interparticle repulsions that can exist between large molecular species (e.g., star polymers) or self-assembled structures (e.g., micelles) in solution.¹¹ The GC fluid is also a compelling model to study because it exhibits several unusual physical properties that are typically associated with molecular or complex-fluid systems with more complicated interactions. For example, at low temperature, the GC fluid displays a re-entrant freezing transition^{4,5,7,10} negative thermal expansivity,^{1,12} and its isothermal compressibility increases upon isobaric cooling.⁶ Although the structural and dynamic properties of the GC fluid are qualitatively similar to those of simpler fluids at low particle concentrations, they become anomalous at sufficiently high particle concentrations. For example, the single-particle dynamics, quantified by, e.g., the self diffusivity, become progressively faster upon increasing particle concentration (diffusivity anomaly).^{6,8,9,12} The static pair correlations,^{2,3,5,6,7,8,9,10} quantified by, e.g., the two-body excess entropy $s^{(2)}$, also weaken upon increasing particle concentration (structural anomaly).⁹

The differences between the structural behavior of the GC fluid at low versus high particle concentration can be qualitatively understood by considering the Gaussian form of the repulsion. At low concentration and low temperature, the average interparticle separation is larger than the range of the interaction. Thus, the part of the GC potential that the particles typically sample when

they “collide” is steeply repulsive. Under these conditions, small increases in concentration lead to the build up of short-range static correlations (i.e., coordination shell structure), similar to what occurs in the hard-sphere fluid.^{2,3,5,6,7,8,9,10} However, at sufficiently high concentration, the bounded form of the GC potential allows the average interparticle separation to become much smaller than the range of the interaction. As a result, particles are effectively penetrable and constantly experience soft repulsive forces from many neighbors. These forces largely cancel one another, creating a “mean field”. Further increasing the concentration only makes this effect more pronounced, paradoxically driving the high-density system toward an ideal-gas-like structure.^{2,3,5,6,7,8,9,10}

Less is understood about the microscopic origins of the anomalous relationship between diffusivity and particle concentration, although the results of recent investigations indicate that the unusual dynamical trends are closely linked to the aforementioned structural anomalies.^{8,9} In particular, the equilibrium GC fluid exhibits a semi-quantitative scaling relation⁹ between self diffusivity D and the two-body excess entropy $s^{(2)}$. Interestingly, this relationship is “normal” in the sense that it is similar to that observed for a wide variety of simpler fluids that do not exhibit either structural or dynamic anomalies.^{9,13,14,15,16} Stated differently, the diffusivity anomaly of the equilibrium GC fluid disappears when one plots D versus $s^{(2)}$ instead of particle concentration.⁹ Similar trends have also recently been reported for other equilibrium fluids with dynamic and structural anomalies, e.g., models with water-like interactions^{17,18,19} or colloid-like, short-range attractions.^{20,21}

In this paper, we further explore the relationship between structure and dynamics in simple models for com-

plex fluids by studying, via molecular simulation, binary mixtures of GC particles. The fluid phase behavior of these systems has already been studied extensively.²² However, here we present, to our knowledge, the first investigation of the relationships between the static pair correlations of the fluid and the tracer diffusivities of the two components.

Specifically, we study the following questions about how these quantities depend on particle concentration and mixture composition. Are the trends in the tracer diffusivities of the two components of the GC mixture closely coupled? Do they scale in a simple way with a single measure of the overall strength of the pair correlations (e.g., $s^{(2)}$)? Or, alternatively, is there a significant decoupling of the single-particle dynamics of the two species? If this latter scenario holds, do the resulting trends in tracer diffusivities track decoupled, species-dependent measures of static structure? Finally, what are the implications of the answers to the above for the compositional dependencies of structural order and tracer diffusivity at low versus high particle concentration?

To address these questions, we use molecular dynamics simulations to investigate equilibrium two-component fluid mixtures of particles that interact via pair potentials of the GC form, $\phi_{ij}(r) = \epsilon_{ij} \exp[-(r/\sigma_{ij})^2]$. Here, r is the interparticle separation, and the parameters ϵ_{ij} and σ_{ij} characterize the energy scale and range of the interactions, respectively, between particles of type i and j with $i, j \in \{A, B\}$. Since we want to understand the behavior of uniform binary fluids, we assign numerical values to the parameters that favor mixing. Specifically, we adopt a set²² introduced earlier ($\sigma_{BB} = 0.665\sigma_{AA}$; $\sigma_{AB} = (0.5[\sigma_{AA}^2 + \sigma_{BB}^2])^{0.5}$; $\epsilon_{AA} = \epsilon_{BB}$; $\epsilon_{AB} = 0.944\epsilon_{AA}$), in which the σ_{ij} were chosen to mimic binary mixtures of self-avoiding polymers in solution.³ We truncate all pair potentials at an interparticle separation of $3.2\sigma_{AA}$, and treat the particles of the two species as having equal masses ($m_A = m_B$).

We carry out the simulations in the microcanonical ensemble, numerically integrating Newton's equations of motion with the velocity-Verlet scheme²³ using a time step of $0.05\sqrt{m_A\sigma_{AA}^2/\epsilon_{AA}}$. We use $N = 3000$ GC particles and a periodically replicated simulation cell, the volume V of which is chosen to realize specific values of reduced total concentrations (i.e., particle densities) in the range $0.05 \leq \rho\sigma_{AA}^3 \leq 1$, where $\rho = N/V$. We investigate mixtures over a wide range of composition ($0.1 \leq x_A \leq 0.9$, where x_A is the mole fraction of species A) and reduced temperature ($0.05 \leq k_B T/\epsilon_{AA} \leq 0.40$). To characterize the single-particle dynamics of species i , we compute its tracer diffusivity D_i by fitting the long-time ($t \rightarrow \infty$) behavior of its average mean-squared displacement $\langle \Delta r_i^2 \rangle$ to the Einstein formula, $D_i = \langle \Delta r_i^2 \rangle / 6t$.²⁴

We compute the two-body excess entropy $s^{(2)}$ directly from the partial radial distribution functions $g_{ij}(r)$ of the fluid using the expression,^{25,26}

$$s^{(2)} = \sum_i x_i s_i^{(2)} \quad (1)$$

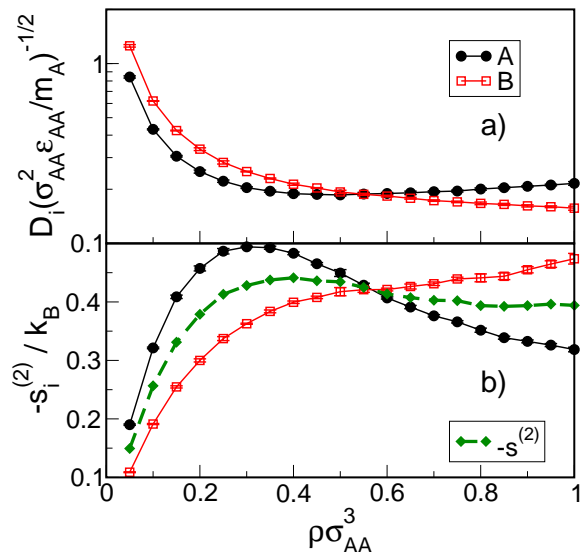


FIG. 1: (a) Tracer diffusivity D_i and (b) structural order metric $-s_i^{(2)}$, with $i \in \{A, B\}$, versus concentration $\rho\sigma_{AA}^3$ for the binary Gaussian-core fluid mixture discussed in the text. The collective structural order metric $-s^{(2)}$ is also included in (b). The temperature is $k_B T/\epsilon_{AA} = 0.1$ and the mole fraction is $x_A = 0.5$.

where $s_i^{(2)}$ is given by

$$\frac{s_i^{(2)}}{k_B} = - \sum_j \frac{x_j \rho}{2} \int [g_{ij}(\mathbf{r}) \ln g_{ij}(\mathbf{r}) - g_{ij}(\mathbf{r}) + 1] d\mathbf{r} \quad (2)$$

Both $-s^{(2)}$ and $-s_i^{(2)}$ are non-negative and can be viewed as translational structural order metrics.²⁷ The former characterizes the overall strength of the pair correlations in the fluid,²⁷ while the latter quantifies the amount of pair structuring surrounding particles of type i .

The first issue that we investigate using our simulation data is how closely the single-particle dynamics of the two species are coupled. Figure 1(a) shows how the computed tracer diffusivities, D_A and D_B , depend on density $\rho\sigma_{AA}^3$ for an equimolar ($x_A = 0.5$) mixture at a temperature of $k_B T/\epsilon_{AA} = 0.1$. As can be seen, D_A follows the same type of non-monotonic trend observed for the self diffusivity of the single-component GC fluid,⁹ displaying an anomalous dependency on particle concentration [$(\partial D_A / \partial \rho)_{T, x_A} > 0$] for densities greater than $\rho\sigma_{AA}^3 \approx 0.4$. On the other hand, D_B shows behavior consistent with that of simple fluids, monotonically decreasing with $\rho\sigma_{AA}^3$ over the density range examined here. The fact that D_A and D_B decouple in this way gives rise to a dynamic crossover density, above which the larger A particles exhibit higher mobility than the smaller B particles. It also suggests that one cannot trivially correlate both the D_A and D_B trends with a single, collective measure of structural order for the fluid, such as $s^{(2)}$ [see, e.g., Fig. 1(b)], a point we examine further below.

Does increasing particle concentration result in a corresponding decoupling of species-specific structural metrics

that, in turn, correlate with the dynamical trends of A and B particles? To examine this possibility, we first plot in Fig. 1(b) the density dependencies of $-s_A^{(2)}$ and $-s_B^{(2)}$. As can be seen, there is indeed a structural decoupling. While both $-s_A^{(2)}$ and $-s_B^{(2)}$ increase with density at low values of $\rho\sigma_{AA}^3$, the increase in ordering is initially more pronounced for the structure surrounding the A particles. This is to be expected because A particles have larger effective contact diameters with their neighbors, and thus respond by building up stronger static pair correlations at low density. However, the large size of the A particles, coupled with the bounded nature of the GC interaction, means that A particles are also forced into more inter-particle overlaps than the B particles as the density is increased. This ultimately leads to a weakening of the static correlations (i.e., coordination shell structure) of the A particles, and hence a maximum in $-s_A^{(2)}$ at an intermediate value of $\rho\sigma_{AA}^3$. As should be expected based on the smaller size of the B particles, a maximum in $-s_B^{(2)}$ (and a corresponding minimum in D_B) can also occur at significantly higher densities, if phase separation of the mixture does not occur first.²⁸ Interestingly, similar to what is observed for the tracer diffusivities, one of the consequences of the $s_i^{(2)}$ decoupling described above is the presence of a structural crossover density above which the smaller B particles exhibit stronger pair correlations than the larger A particles.

The data in Fig. 1(a) and (b) suggests a negative correlation between D_A and $-s_A^{(2)}$ (and also between D_B and $-s_B^{(2)}$), in which the structural crossover ($s_A^{(2)} = s_B^{(2)}$) occurs at approximately the same density as the dynamic crossover ($D_A = D_B$). In fact, although we focus on one particular pairing of composition and temperature in Fig. 1, these trends are exhibited by this system for a wide range of compositions and temperatures (see the supplementary Fig. 4)

To quantitatively examine the correlation between single-particle dynamics and structure, we studied possible generalizations of a scaling relationship that describes the behavior of the single-component GC fluid. In the case of the single-component fluid, the so-called Rosenfeld scaled¹⁴ self diffusivity $D^R = D\rho^{1/3}(k_B T/m_i)^{-1/2}$ is approximately a single-valued function of $-s^{(2)}$ across a wide range of temperature and density.⁹ Figure 2(a), however, shows that a naïve extension of this result for mixtures, $D_i^R = D_i\rho^{1/3}(k_B T/m_i)^{-1/2}$ versus $-s^{(2)}$, does not adequately collapse the data for either of the two species. This should not be particularly surprising, given the dynamical and structural decouplings shown in Fig. 1(a) and (b).

On the other hand, Figure 2(b) examines a species-specific extension of the single-component scaling law, D_i^R versus $-s_i^{(2)}$. Interestingly, not only does this generalization collapse the temperature, density, and compositional dependencies of tracer diffusivity for each individual particle type, but the behaviors of the two species are, to a good approximation, accounted for by the math-

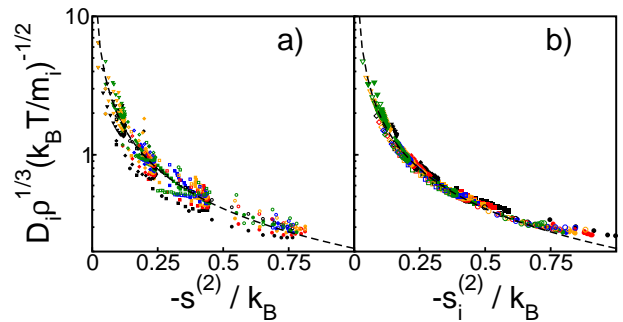


FIG. 2: Rosenfeld scaled tracer diffusivity $D_i^R = D_i\rho^{1/3}(k_B T/m_i)^{-1/2}$ versus (a) two body excess entropy $-s^{(2)}$ and (b) its contribution from structuring around type i particles $-s_i^{(2)}$, with $i \in \{A, B\}$, for the binary Gaussian-core fluid mixture discussed in the text. Shown are mole fractions $x_A = 0.1$ (black), 0.3 (red), 0.5 (orange), 0.7 (blue), and 0.9 (green) and temperatures $k_B T/\epsilon_{AA} = 0.05$ (\circ), 0.1 (\square), 0.2 (\diamond) and 0.4 (∇). Filled and open shapes represent A and B particles, respectively. The dashed line indicates a least-square fit to a power law relationship for the single-component GC fluid⁹, $D^R = 0.208s^{(2)-0.972}$.

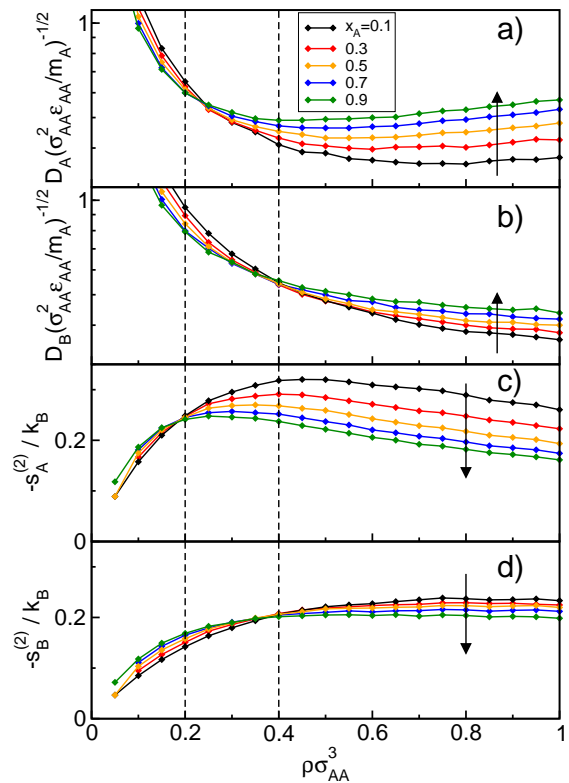


FIG. 3: Tracer diffusivity D_i for (a) A particles and (b) B particles and structural order metric $-s_i^{(2)}$ for (c) A particles and (d) B particles for the binary Gaussian-core mixture discussed in the text. All are plotted versus density $\rho\sigma_{AA}^3$. Data shown is for temperature $k_B T/\epsilon_{AA} = 0.2$ and mole fractions $x_A = 0.1, 0.3, 0.5, 0.7$ and 0.9 . Arrows indicate increasing x_A . The dashed lines separate the approximate low, intermediate and high density ranges described in the text.

ematical form of the scaling law for the single-component GC fluid.

We now explore what this correlation implies about how mixture composition affects the tracer diffusivities [Figure 3(a),(b)] and species-specific pair-correlation contributions to excess entropy [Figure 3(c),(d)]. As should be expected, at low values of density ($\rho\sigma_{AA}^3 < 0.2$), the response of the system to changes in composition is normal, i.e., qualitatively similar to that of simple atomic or hard-sphere-like mixtures where interparticle “collisions” dominate. Under these conditions, increasing the mole fraction of the larger A particles effectively increases the “packing fraction” of the fluid, which in turn decreases the mobility and increases the local structural order surrounding both types of particles.

At high values of density, on the other hand, the fact that the bounded GC potential allows for significant interparticle overlaps changes the physics. Since increasing the mole fraction of the larger particles (at constant density) here increases the number of overlaps and nudges the system toward the mean-field fluid, one expects anomalous behavior in dynamics and structure, i.e. a corresponding increase in D_i and decrease in $-s_i^{(2)}$ for both species. Indeed, Figure 3 shows that these anoma-

lous compositional trends for dynamics and structure do occur for $\rho\sigma_{AA}^3 > 0.4$.

In closing, we note a final manifestation of the decoupled behavior for the two species of this GC mixture. Specifically, the densities at which the compositional trends for structure and dynamics transition from normal to anomalous are significantly different for the two species, with the larger species logically becoming anomalous at a lower overall density. The implication is that there is a fairly wide range of intermediate fluid densities (approximately $0.2 < \rho\sigma_{AA}^3 < 0.4$) for which the structure and dynamics of the A particles behave anomalously, while those of the B particles behave normally, with respect to changes in composition.

Two authors (T.M.T and J.R.E) acknowledge financial support of the National Science Foundation (CTS-0448721 and CTS-028772, respectively). One author T.M.T. also acknowledges support of the Welch Foundation (F-1696) and the David and Lucile Packard Foundation. M.J.P. acknowledges the support of the Thrust 2000 - Harry P. Whitworth Endowed Graduate Fellowship in Engineering. The Texas Advanced Computing Center (TACC) provided computational resources for this study.

-
- * Electronic address: mjp736@che.utexas.edu
 † Electronic address: vincent.shen@nist.gov
 ‡ Electronic address: jerring@buffalo.edu
 § Electronic address: truskett@che.utexas.edu; Corresponding Author
- ¹ F. H. Stillinger and D. K. Stillinger, *Physica A* **244**, 358 (1997).
 - ² A. Lang, C. N. Likos, M. Watzlawek, and H. Lowen, *J. Phys.: Condens. Matter* **12**, 5087 (2000).
 - ³ A. A. Louis, P. G. Bolhuis, and J. P. Hansen, *Phys. Rev. E* **62**, 7961 (2000).
 - ⁴ S. Prestipino, F. Saija, and P. V. Giaquinta, *J. Chem. Phys.* **123**, 144110 (2005).
 - ⁵ P. V. Giaquinta and F. Saija, *Chemphyschem* **6**, 1768 (2005).
 - ⁶ P. Mausbach and H. O. May, *Fluid Phase Equilib.* **249**, 17 (2006).
 - ⁷ C. E. Zachary, F. H. Stillinger, and S. Torquato, *J. Chem. Phys.* **128**, 224505 (2008).
 - ⁸ H. Wensink, H. Löwen, M. Rex, C. Likos, and S. van Teeffelen, *Comput. Phys. Commun.* **179**, 77 (2008).
 - ⁹ W. P. Krekelberg, T. Kumar, J. Mittal, J. R. Errington, and T. M. Truskett, *Physical Review E* **79**, 031203 (2009).
 - ¹⁰ F. H. Stillinger, *J. Chem. Phys.* **65**, 3968 (1976).
 - ¹¹ C. N. Likos, *Physics Reports* **348**, 267 (2001).
 - ¹² F. H. Stillinger and T. A. Weber, *J. Chem. Phys.* **68**, 3837 (1978).
 - ¹³ Y. Rosenfeld, *Phys. Rev. A* **15**, 2545 (1977).
 - ¹⁴ Y. Rosenfeld, *J. Phys.: Condens. Matter* **11**, 5415 (1999).
 - ¹⁵ M. Dzugutov, *Nature* **381**, 137 (1996).
 - ¹⁶ J. Mittal, J. Errington, and T. Truskett, *J. Phys. Chem. B* **111**, 10054 (2007).

- ¹⁷ J. R. Errington and P. G. Debenedetti, *Nature* **409**, 318 (2001).
- ¹⁸ J. Mittal, J. R. Errington, and T. M. Truskett, *J. Chem. Phys.* **125**, 076102 (2006).
- ¹⁹ J. R. Errington, T. M. Truskett, and J. Mittal, *J. Chem. Phys.* **125**, 244502 (2006).
- ²⁰ J. Mittal, J. R. Errington, and T. M. Truskett, *J. Phys. Chem. B* **110**, 18147 (2006).
- ²¹ W. P. Krekelberg, J. Mittal, V. Ganesan, and T. M. Truskett, *J. Chem. Phys.* **127**, 044502 (2007).
- ²² A. J. Archer and R. Evans, *Phys. Rev. E* **64**, 041501 (2001).
- ²³ M. P. Allen and D. J. Tildesley, *Computer Simulations of Liquids* (Oxford University Press, New York, 1987).
- ²⁴ We use Student’s t distribution together with the tracer diffusivities from five independent runs to estimate 95% confidence intervals for the D_i .
- ²⁵ J. Hernando, *Molecular Physics* **69**, 319 (1990).
- ²⁶ A. Samanta, S. M. Ali, and S. K. Ghosh, *Phys. Rev. Lett.* **87**, 245901 (2001).
- ²⁷ T. M. Truskett, S. Torquato, and P. G. Debenedetti, *Phys. Rev. E* **62**, 993 (2000).
- ²⁸ In the limit of pure B ($x_A = 0$), one observes⁹ both $(\partial D_B / \partial \rho)_{T, x_A} > 0$ and $(\partial s_B^{(2)} / \partial \rho)_{T, x_A} > 0$ for reduced densities greater than $\rho\sigma_{AA}^3 \approx 1.4$. However, we have found in our studies of this system that, for non-zero values of x_A , the binary GC fluid will often phase separate at densities below where the onset of anomalous dynamic and structural behavior occurs.

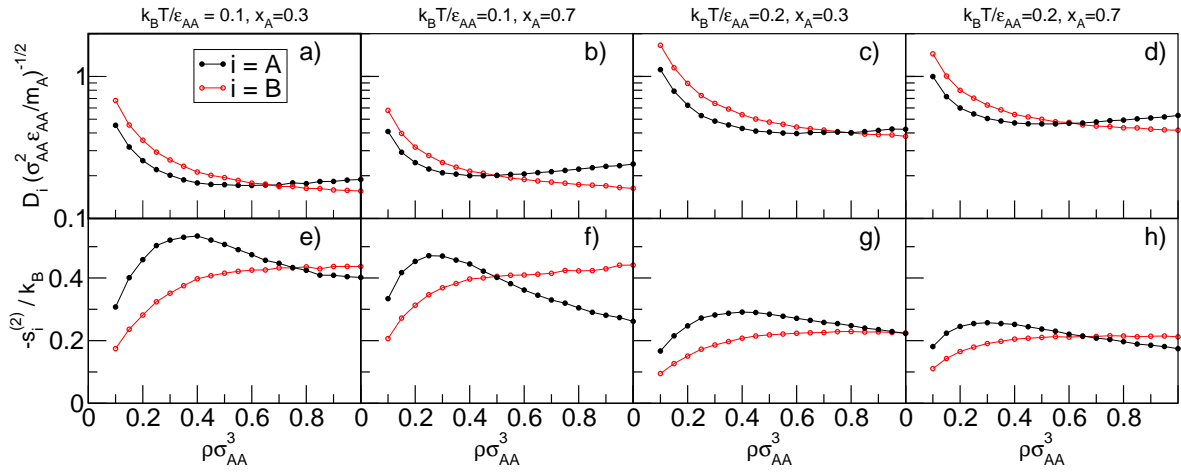


FIG. 4: (a-d) Tracer diffusivity D_i and (e-h) structural order metric $-s_i^{(2)}$, with $i \in \{A, B\}$, versus concentration $\rho\sigma_{AA}^3$ for the binary Gaussian-core fluid mixture discussed in the text. The columns are systems at different temperatures and mole fractions, which are listed above the respective column.